Respiratory Research

RESEARCH

Open Access

Modulation of the Epithelial–mesenchymal transition process by Forkhead Box C2 in the repair of airway epithelium after injury

Yudong Wang[1] and Jun Liu[1*]

Abstract

Background Epithelial–mesenchymal transition (EMT) is regarded as a key process in repair of airway epithelium after injury. Forkhead Box C2 (FOXC2) is a transcription factor involved in EMT process, whether it is involved in repair of bronchial epithelium remains unknown.

Methods C57BL/6 mice were subjected to intraperitoneal injection with naphthalene (NAPH; 200 mg/kg) to induce airway injury model. qPCR, immunoblot and FOXC2 immunohistochemistry assays were conducted to detect the expression of FOXC2 in bronchial epithelium. To explore the function of FOXC2 in NAPH-induced airway injury, the mice were given intratracheal administration of shFOXC2- or shNC-lentivirus particles, followed by NAPH treatment. Hematoxylin-and-eosin staining was used to assess the histopathology of the bronchial epithelium. Immunofluorescence analysis of CCSP, a club cell marker confirmed the CCSP expression in bronchial epithelium. Immunoblot and immunofluorescence assays determined the expression of E-cadherin, vimentin, and N-cadherin. In mouse primary bronchial epithelial cells (PBECs), we overexpressed and silenced FOXC2 by lentivirus particles, respectively. Cell migration was analyzed using wound healing assay. Immunoblot assays determined the E-cadherin, vimentin, FN-EDA expression in TGF-β1-induced PBECs. mRNA sequencing (mRNA-seq) and FOXC2 ChIP sequencing (ChIP-seq) to reveal the downstream genes of FOXC2 in TGF-β1-induced PBECs. Luciferase assay, ChIP-PCR and functional rescue experiments were performed to confirm the interaction of FOXC2/formin binding protein 1 (FNBP1) in TGF-β1-induced PBECs.

Results FOXC2 expression was up-regulated in the lung tissues of mice at 2, 3 and 6 days post-NAPH. FOXC2 knockdown in bronchial epithelium of mice delayed $CCSP^+$ club cell regeneration and normal repair of the airway epithelium within 14 days after injury. Knockdown of FOXC2 increased E-cadherin but decreased vimentin and N-cadherin, EMT markers during early phase after injury. In vitro, knockdown of endogenous FOXC2 repressed the migration of cells and increased TGF-β1-induced E-cadherin but decreased vimentin, N-cadherin and FN-EDA. Exogenous FOXC2 addition exerted opposite effects. Furthermore, mRNA-seq and FOXC2 ChIP-seq revealed that FNBP1 might be a downstream target of FOXC2. Overexpression of FNBP1 reversed the inhibitory role of FOXC2 knockdown in EMT.

Conclusions These data highlight the important function of FOXC2 as a regulator in repair of bronchial epithelium after injury.

Keywords NAPH, Airway repair, Epithelial–mesenchymal transition, FOXC2, FNBP1

*Correspondence:
Jun Liu
jliu74@cmu.edu.cn

Graphical Abstract

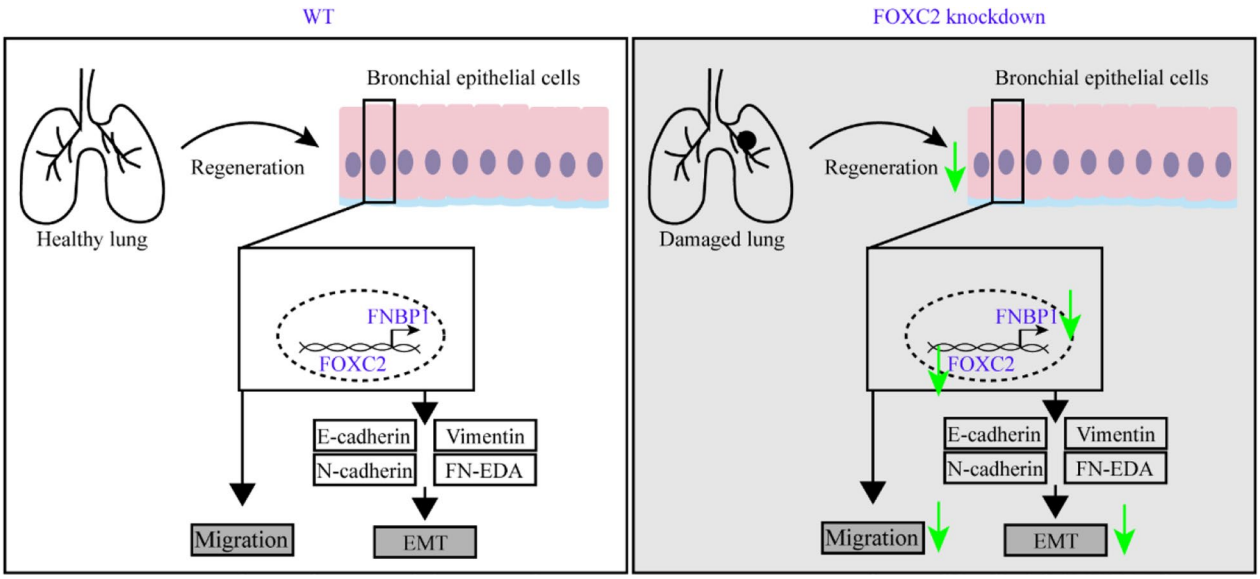

Introduction

Airway epithelium plays pivotal roles in the defense against allergens, pathogens and pollutants in the air. Airway remodeling characterized by structural changes is produced by epithelial injury and repair in chronic lung diseases including pulmonary fibrosis, asthma and emphysema [1, 2]. Exploring the molecular mechanism of defective epithelium repair in airway remodeling is of tremendous importance for the prevention or treatment of chronic lung diseases.

Naphthalene (NAPH) is an acute toxicant, which causes airway damage during a short period of time [3]. Club cells are a secretory epithelial cell type that located in the bronchial epithelium. In chronic lung diseases, club cells contribute to the repair after epithelium injury by self-renewal and differentiation [4]. In NAPH-induced injury in mice, the vacuolar club cells are immediately dead and exfoliated at 24 h. Surviving cells have a major responsibility of the airway repair. Cell migration is obviously increased at 2–3 days after injury due to a morphological Epithelial–mesenchymal transition (EMT). Cell differentiation occurs at 6–7 days post-NAPH. By 14 days post-injury, the injury is largely complete [3, 5]. However, the molecular mechanisms of bronchial epithelium repair have not been elaborated.

Forkhead Box C2 (FOXC2) is a member of the FOX transcription factor family, which is involved in multiple biological processes, including cell migration and tissue regeneration. In human diseases, FOXC2 controls the development of the disease process through several mechanisms, including EMT and cell migration [6–8]. There is also evidence that deletion of FOXC2 aggravates ischemia/reperfusion-induced intestinal damage [9]. FOXC2 in the injured tubular cells has been found to active EMT process [10]. In the development of the lung, FOXC2 knockout causes the aberrant differentiation of alveolar epithelial cells [11]. However, the function of FOXC2 in bronchial epithelium in response to NAPH-induced injury remains unknown.

In the current study, we found that FOXC2 is highly expressed in bronchial epithelium of mice with NAPH exposure. Knockdown of FOXC2 causes defective repair of bronchial epithelium in vivo. In vitro studies suggest that FOXC2 enhances epithelial wound responses using mouse primary bronchial epithelial cells (PBECs). mRNA sequencing (mRNA-seq) and ChIP sequencing (ChIP-seq) and the related functional assays reveal that formin binding protein 1 (FNBP1) may be a downstream target of FOXC2. FNBP1, a member of the F-Bar protein family, has been documented to influence cell survival, EMT and migration [12–14]. A down-regulated expression of FNBP1 in response to FOXC2 indicated that FOXC2 via FNBP1 might play a key role in bronchial epithelial wound repair. Our data highlight that FOXC2 is a key transcription factor involved in bronchial epithelial wound repair by regulating FNBP1 transcription.

Materials and methods

Plasmids and shRNA constructs

The cDNA encoding *Mus* FNBP1 (NM_001177648), or cDNA encoding *Mus* FOXC2 (NM_013519), or FOXC2 shRNA^{-1} (5′-CCTACAACATGTTCGAGAATG-3′), or FOXC2 shRNA^{-2} (5′-CCTTCTACCGCGAGAACA AGC-3′) was amplified and then inserted into the pLVX-IRES-puro vector or pLVX-shRNA1 vector (Fenghui Shengwu, Changsha, China). For lentivirus production, the vector along with lentiviral packaging pSPAX2 vector and envelope pMD2.G vector (Fenghui Shengwu, Changsha, China) were co-transfected into HEK293T cells (Cellverse, Shanghai, China) using Lipofectamine 3000 transfection reagent (Invitrogen, CA, USA). Lentivirus was harvested 48 h and 72 h following transfection.

Airway epithelial injury induction and treatment

A total of 120 eight-week-old female C57BL/6 mice were kept in suitable mouse cages with free access to food and water for 1 week before experiment. Animal experimental protocol was approved by the Shengjing Hospital of China Medical University Institute Animal Care and Use Committee (approval number: 2024PS116K).

NAPH (CAS number 91–20-3) was purchased from Shanghai Macklin Biochemical Technology Co., Ltd (Shanghai, China). NAPH-induced airway epithelial injury in C57BL/6 mice was conducted according to the method of Gorissen et al. [5]. The mice in NAPH group were subjected to intraperitoneal injection of 200 mg/kg NAPH in corn oil. Control mice were injected with corn oil. At 1, 2, 3, 6, and 14 days after NAPH injection, lung tissues were harvested for analysis. For in vivo experiments, experiments were accomplished with n = 6 randomized animals per group.

To explore the role of FOXC2 in airway injury repair, mouse trachea was exposed by making a cervical incision under anesthesia, the mice were intratracheally infected of lentiviral particles (3×10^6 TU) 3 days before NAPH treatment. At 3, 6, and 14 days after NAPH treatment, lung tissues were collected for subsequent assays.

Histopathology of lung tissues

The lung tissue samples were fixed in 4% paraformaldehyde overnight at 4 °C. The tissues were embedded in paraffin, sectioned into 5 μm thick sections and stained with hematoxylin (Solarbio, Beijing, China) and eosin (Sangon, Shanghai, China). The staining results were observed with an Olympus DP73 microscopy (Olympus, Tokyo, Japan; magnification, × 200).

Immunohistochemistry

FOXC2 expression in lung tissues was detected by standard immunohistochemistry assay. The antigen repair solution was put into a heat-resistant container and heated in the microwave oven until boiling. Then, the prepared samples were placed in the antigen repair solution and heated for 10 min for antigen repair. After antigen retrieval, 3% H_2O_2 incubation and 1% BSA incubation, the sections were immunostained with mouse FOXC2 antibody (1:100; Bioss, Beijing, China) overnight at 4 °C. Incubation of the secondary antibody (HRP-labeled goat anti-rabbit IgG; 1:200; Sangon, Shanghai, China) were performed for 1 h at room temperature. The color was developed using Diaminobenzidine (DAB; Solarbio, Beijing, China) chromogen and nuclei counterstain was achieved with hematoxylin. The staining images were captured by an Olympus DP73 microscopy (magnification, × 400).

Immunofluorescence

For single immunofluorescence staining of lung tissues, the lung sections were incubated overnight with club cell secretory protein (CCSP) primary antibody (1:50; Santa Cruz, CA, USA) at 4 °C. The lung sections were then incubated with anti-mouse IgG secondary antibody (1:200; CST, MA, USA) for 1 h. For single immunofluorescence staining of PBECs, the cells were seeded on glass slides in a cell culture plate, and the fixed cells with 4% paraformaldehyde were incubated overnight with vimentin primary antibody (1:100; Affinity, Changzhou, China) at 4 °C. The cell slices were then incubated with anti-rabbit IgG secondary antibody (1:200; CST, MA, USA) for 1 h. For double immunofluorescence staining, the lung sections were incubated with primary antibodies anti-CCSP (1:50; Santa Cruz, CA, USA) and anti-vimentin (1:100; Affinity, Changzhou, China) or anti-N-cadherin (1:100; Affinity, Changzhou, China). The secondary antibodies anti-rabbit IgG and anti-mouse IgG (1:200; CST, MA, USA) was used and the incubation time was 1.5 h. DAPI (Aladdin, Shanghai, China) was used for counterstain. All slides were mounted on microscopy and staining results were analyzed with the Olympus DP73 microscopy (magnification, × 400).

Cell culture and treatment

Mouse PBECs was purchased from Cellverse Bioscience Technology Co., Ltd (Shanghai, China). Cell culture was conducted according to the manufactures instructions (in a 37 °C, 5% CO_2 incubator). Air–liquid interface (ALI) culture of PBECs was performed as described previously [15]. In this study, PBECs were grown in ALI culture system (Cellverse, Shanghai, China) for 21 days for cell differentiation. For exploring the role of FOXC2 in vitro, PBECs were infected with the indicated lentivirus particles at a multiplicity of infection (MOI) of 20, including lv-shFOXC2, lv-shNC, lv-FOXC2oe (lentivirus

overexpressing FOXC2), or lv-Vector (empty Vector). After 72 h of infection, some cells were subjected to wound healing assay. Other cells were treated with recombinant TGF-β1 (SinoBiological, Beijing, China; 10 ng/ml) for 24 h. In addition, PBECs were infected with lv-shFOXC2 and lv-FNBP1oe (lentivirus overexpressing FOXC2) for 72 h, followed by TGF-β1 treatment.

Luciferase assay

Human 293 T cells were kept in DMEM (Servicebio, Wuhan, China) including 10% FBS (Bioshrap, Anhui, China). Cells were transfected with FOXC2 overexpression plasmid (FOXC2oe) or the control (pcDNA-3.1) and FNBP1 promoter luciferase reporter vectors using the Lipofectamine 3000 (Invitrogen, CA, USA). At 48 h after transfection, luciferase activity was measured using a dual luciferase reporter assay kit (KeyGen, Nanjing, China) following the manufacturer's protocols.

Wound healing assay

Cell migratory ability was tested with a wound healing assay. The infected cells were cultured in serum-free medium and scratched using a 200 μl pipette tip. At 0 h and 24 h after scratching, the wounded areas were captured under the Olympus DP73 microscopy (magnification, × 100) and the percentage of wound closure was calculated.

Quantitative PCR assay

The expression of FOXC2 and FNBP1 mRNA in lung tissues or PBECs was determined by quantitative PCR (qPCR). Total RNA was extracted with TRIpure lysis buffer (Bioteke, Beijing, China). The first-strand cDNA was synthesized with All-in-One First-Strand Super-Mix (Magen, Guangzhou, China) following the manufacturer's instructions. qPCR assay was performed with SYBR Green (Solarbio, Beijing, China) in accordance with the manufacturer's protocols. The primers utilized were as follows: FOXC2 forward, 5′-GAACAGCAT CCGCCACA-3′ and reverse, 5′-CCGCTCCTCCTT GTCCTT-3′; FNBP1 forward, 5′-AGTGCCTGGACG GGATA-3′ and reverse, 5′-GCGTTTCATTGGCTGTG-3′; and β-actin forward, 5′-CATCCGTAAAGACCTCTA TGCC-3′ and reverse, 5′-ATGGAGCCACCGATCCAC A-3′.

Chromatin immunoprecipitation and PCR assay

ChIP assay was performed using a ChIP assay kit (Beyotime, Shanghai, China) as per the manufacturer's instructions. Protein-DNA complexes were overnight incubated with anti-FOXC2 antibody or IgG. Whole cell lysate was used as Input control. After washing, the effectiveness of ChIP was evaluated by PCR assay. The primers used were: FNBP1 forward, 5′-ACATTCCCGAGTTCTTTC C-3′ and reverse, 5′-TCGCCATCTGCCTTCTAC-3′.

Immunoblot assay

Total protein was extracted using cell lysis buffer (Beyotime, Shanghai, China) and BCA kit (Beyotime, Shanghai, China) was used for quantification of protein concentration. Proteins were separated using 10% SDS-PAGE and then transferred onto PVDF membranes (Abcam, Cambridge, UK) for 30 min. After blocking for 1 h with blocking solution (Beyotime, Shanghai, China), the membranes were overnight incubated at 4 °C with anti-FOXC2 antibody (1:100; Santa Cruz, CA, USA), anti-E-cadherin, anti-vimentin, anti-N-cadherin antibody (1:1000; Affinity, Changzhou, China), or anti-cellular fibronectin (FN-EDA) antibody (1:2000; Proteintech, Wuhan, China). The secondary antibodies (goat anti-mouse or anti-rabbit IgG-HRP; 1:1000; Beyotime, Shanghai, China) were applied for an incubation of 45 min. The blots were observed using ECL solution (Beyotime, Shanghai, China).

mRNA sequencing and ChIP sequencing

mRNA-seq and ChIP-seq analyses were performed according to the previous description [16]. For gene expression profile, the RNA was extracted from PBECs and cDNA libraries were prepared. An illumina sequencing platform was used for mRNA-seq. R language package DESeq2 was used to determine the differential gene expression. For ChIP-seq of FOXC2, PBECs were incubated with anti-FOXC2 antibody or IgG. The precipitated DNA was extracted and purified for Illumina sequencing.

Bioinformatics analysis

The GSE17693 dataset was obtained from the Gene Expression Omnibus (GEO) database (http://www.ncbi.nlm.nih.gov/geo/). The criterion of $|Log_2FC| > 1$ and $p < 0.05$ was used to screen the differentially expressed genes (DEGs). EMT-related genes were screened using GeneCards database (https://www.genecards.org).

Statistical analysis

Values are presented as mean ± standard deviation (SD). Statistical analysis was conducted by GraphPad Prism 8.0 software. Differences were evaluated using Student's t-test or analysis of variance (ANOVA). $P \leq 0.05$ was regarded as statistically significant.

Results

FOXC2 is highly expressed in the lungs of NAPH-treated mice

Based on the GSE17693, a dataset related with repair of airway epithelium after injury, we obtained gene

expression profiles of the lung samples from the mice with NAPH treatment (6 days post-NAPH) and healthy control. According to the screening criterion of $|Log_2FC| > 1$ and $p < 0.05$, we identified 2585 up-regulated DEGs and 1341 down-regulated DEGs (Fig. 1A and B). Transcription factors (TFs) are the key regulators involved in transcriptional regulation and plays crucial roles in multiple biological processes, including EMT. The members of FOX transcription factor family are mostly important in the modulation of cell migration and EMT [17–19]. Thus, we specifically focused on the forkhead box family in this study. Figure 1C displayed the DEGs belong to FOX transcription factor family depicted as a Heat-map. Of these 11 DEGs, FOXL1 has been reported to play a primary role in lung fibroblasts [20], and FOXJ1 has been found to modulate the repair of airway epithelium [17]. The third DEG, FOXC2, was selected in this study. GO enrichment analysis revealed that FOXC2 might be involved in the regulation of cell differentiation, migration and tissue remodeling (Fig. 1D). Further analysis of the GSE17693 dataset found that the expression of FOXC2 was up-regulated in response to NAPH-induced airway epithelium injury at various time points (Fig. 1E), implying the importance of FOXC2 in injury repair. To confirm the above findings, airway injury in mice was induced by NAPH intraperitoneal injection (Fig. 2A). qPCR and immunoblot results demonstrated that FOXC2 expression was up-regulated to varying degrees in the lungs of

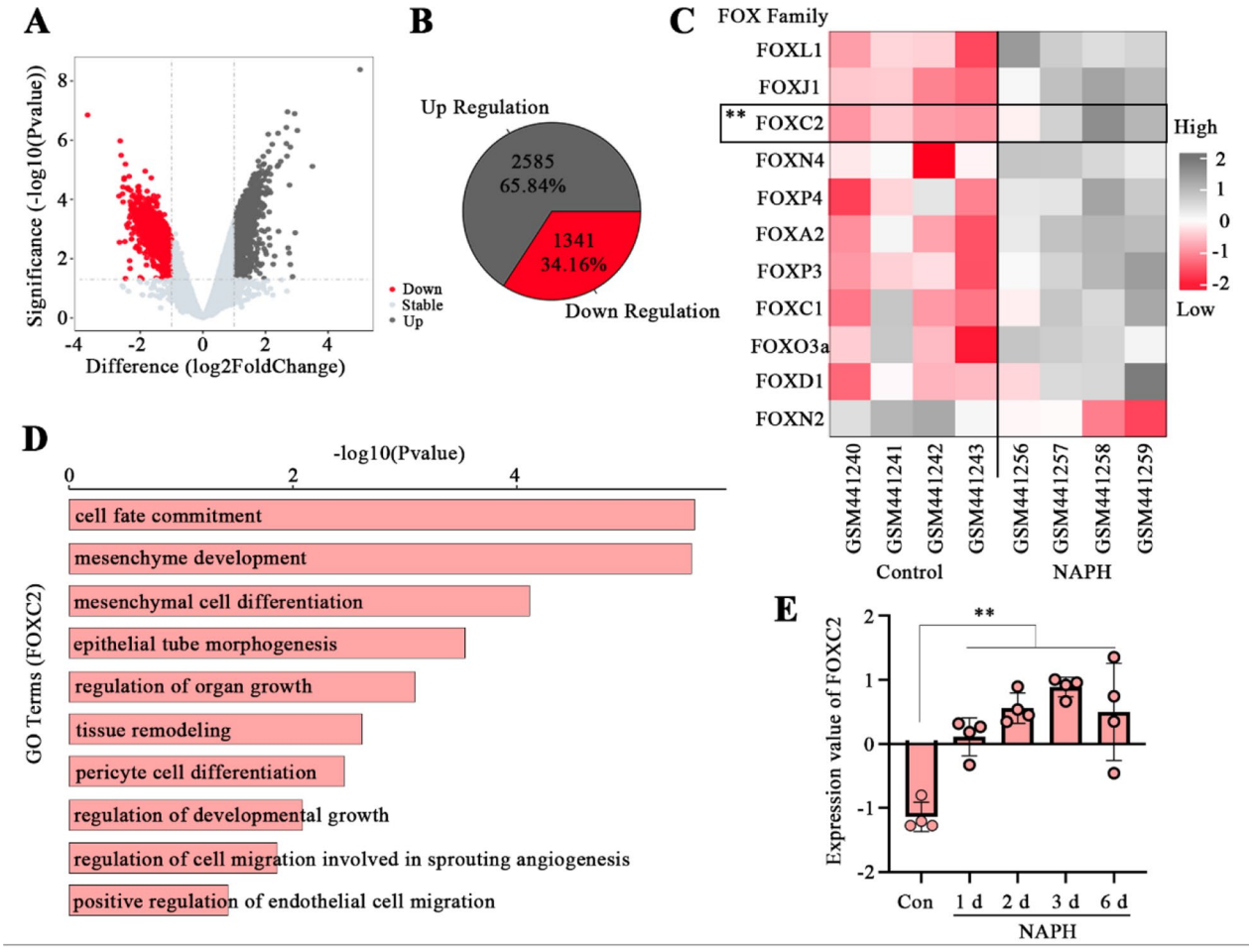

Fig. 1 Online database analysis of FOXC2 expression in the NAPH model of airway injury. **A** Differentially expressed genes (DEGs) in GSE17693 were shown with a volcano map using |Log2FC|> 1 and $p < 0.05$ as the screening criterion. Red indicates down-regulated DEGs, and dark grey indicates up-regulated DEGs. **B** Pie chart showed the number and percentage of up- and down-regulated DEGs in naphthalene (NAPH)-treated lung tissues compared with the control group. **C** Heat-map analysis of FOX (Forkhead Box) transcription factor family. **D** Gene Ontology (GO) functional annotation analysis of FOXC2. **E** FOXC2 expression value in the lung tissues of control mice and NAPH-treated mice. Data are presented as mean ± SD. **$p < 0.01$

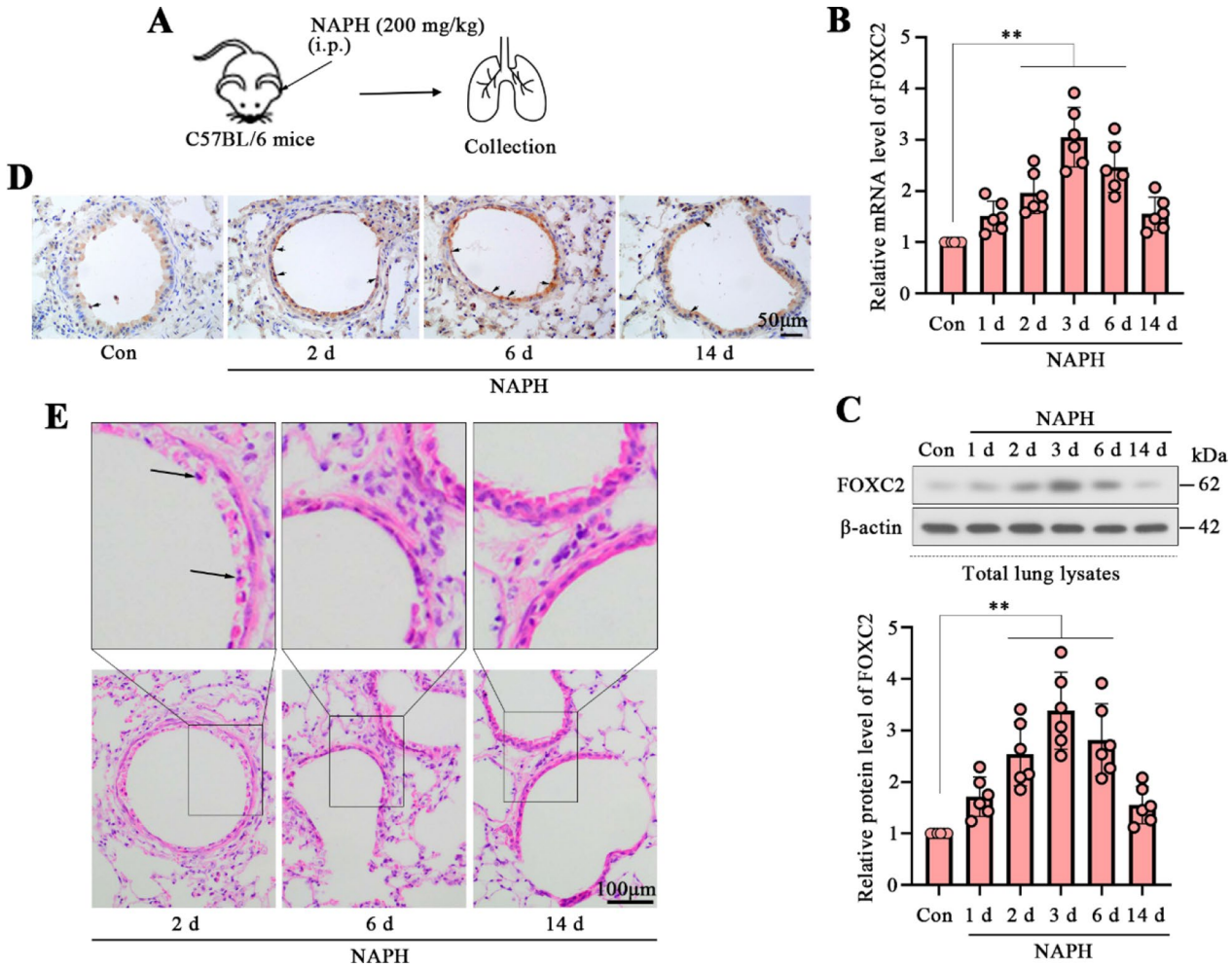

Fig. 2 FOXC2 expression is up-regulated in NAPH-treated mice. **A** Female C57BL/6 mice were subjected to intraperitoneal injection with 200 mg/kg NAPH, and lung tissues were harvested for subsequent analysis at indicated time points. **B** qPCR analysis of FOXC2 were performed in the lung tissues. **C** Immunoblots were carried out for FOXC2. **D** Representative FOXC2 immunohistochemistry of lung tissues. Black arrows indicate FOXC2-positive staining. Scale bar: 50 μm. **E** The lung tissues were stained with hematoxylin & eosin for morphological observation. Black arrows indicate injured cells. Scale bar: 100 μm. Data are presented as mean ± SD. **p < 0.01

NAPH-treated mice compared with the control, and was significantly up-regulated on days 2, 3, and 6 post-NAPH (Fig. 2B and C). FOXC2 immunohistochemistry results verified the qPCR and immunoblot findings, and showed that FOXC2 was expressed in the bronchial epithelium (Fig. 2D). Hematoxylin-and-eosin staining uncovered that there were injured and exfoliated cells in bronchial epithelium on day 2 post-NAPH. By days 6 and 14 post-NAPH, there was gradual regeneration of epithelial cells (Fig. 2E).

FOXC2 affects airway epithelial regeneration in NAPH-treated mice

To determine the function of FOXC2 in bronchial epithelium repair in vivo, the lentivirus-mediated knockdown of FOXC2 in the bronchial epithelium was administrated in NAPH model of airway injury (Fig. 3A). qPCR and immunoblot analysis showed obvious suppression of FOXC2 mRNA and protein by lentivirus-mediated shFOXC2 (Fig. 3B and C). An analysis of immunohistochemistry revealed the decreased FOXC2 protein in the bronchial epithelium after lv-shFOXC2 administration at 3 days post-NAPH (Fig. 3D). By day 14, NAPH-induced cell injury gradually repaired and the airway changes reversed back to the basal level, while knockdown of FOXC2 caused delayed epithelial regeneration, demonstrated by exfoliated epithelial cells, as described in Fig. 3E. Immunofluorescence analysis of CCSP, a club cell marker showed

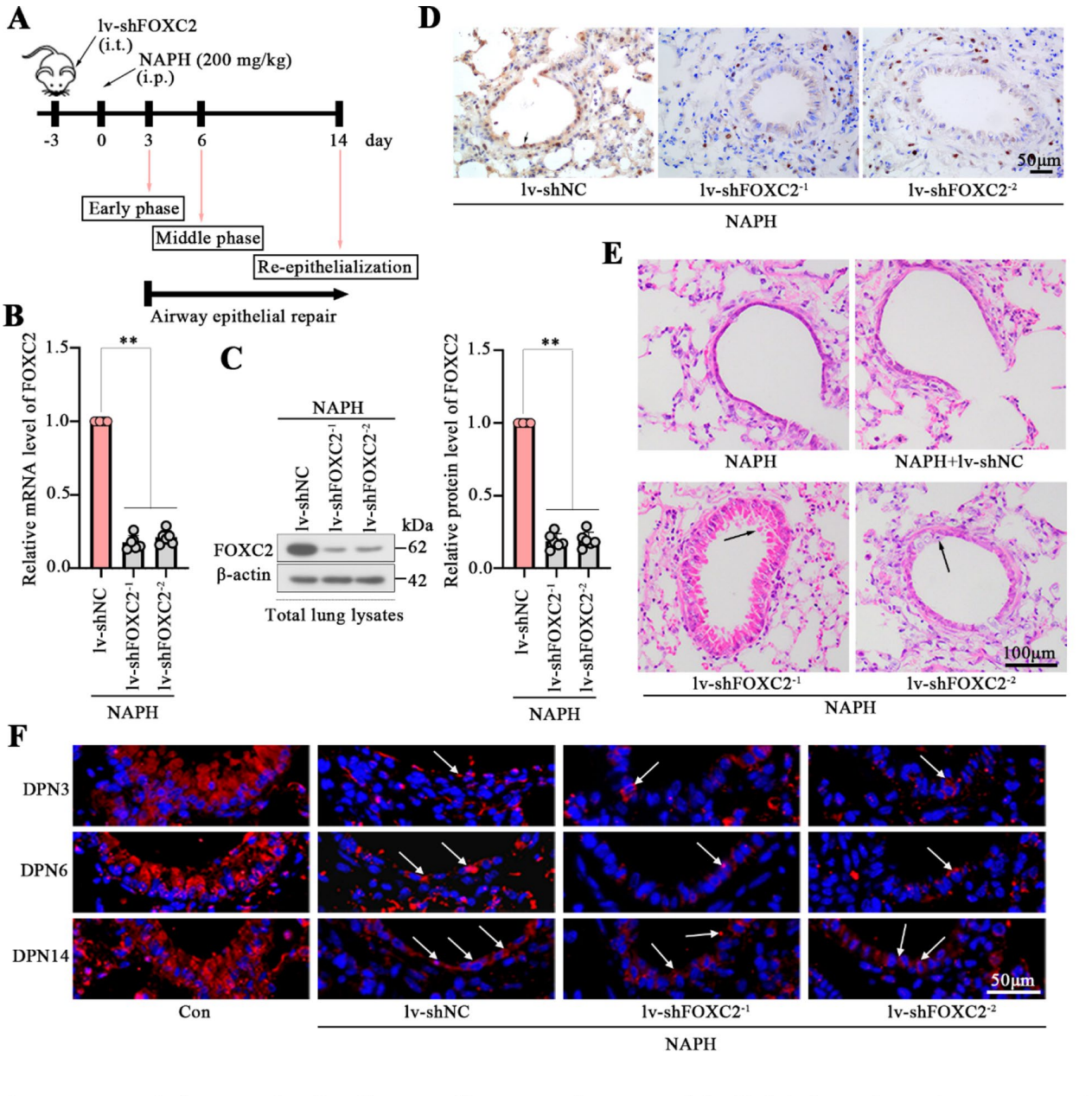

Fig. 3 Knockdown of FOXC2 ameliorates airway epithelial injury in NAPH-treated mice. **A** Experimental diagram of in vivo experiments. **B**, **C** FOXC2 expression in the lung tissues by qPCR and immunoblot analysis. **D** Immunohistochemistry indicated the expression of FOXC2 in the bronchiolar epithelium of lung tissues. **E** Morphological observation of the lung tissues at 14 days post-NAPH using hematoxylin & eosin staining. Black arrows indicate injured cells. **F** Club cells in the lung tissues were stained with an anti-CCSP antibody, and representative immunofluorescence images were displayed. White arrows indicate CCSP-positive cells. Scale bar: 50 μm. DPN: days post NAPH. Data are presented as mean ± SD. $^{**}p < 0.01$

that at 3 days post-NAPH, $CCSP^+$ club cells were lost, while returned to normal levels at 14 days post-NAPH. FOXC2 knockdown had no significant effect on club cell number induced by NAPH at 3 days post-NAPH, but delayed the differentiation of club cells at 6 days post-NAPH, causing the delay of repair within 14 days after injury (Fig. 3F).

FOXC2 knockdown regulates the expression of EMT markers in response to NAPH-induced airway epithelial injury

EMT is a key process for tissue regeneration [21]. Immunoblot assays were performed to determine the expression of EMT markers E-cadherin, vimentin, and N-cadherin in the lung tissues. We found an obvious reduction in E-cadherin and increase in vimentin and N-cadherin in the lungs of NAPH-treated mice. In response to FOXC2 knockdown, there were increased E-cadherin and decreased vimentin and N-cadherin in the lungs (Fig. 4A). Immunofluorescence results of vimentin and N-cadherin indicated the reduced vimentin and N-cadherin expression in the bronchial epithelium of NAPH-treated mice with FOXC2 knockdown (Fig. 4B and C).

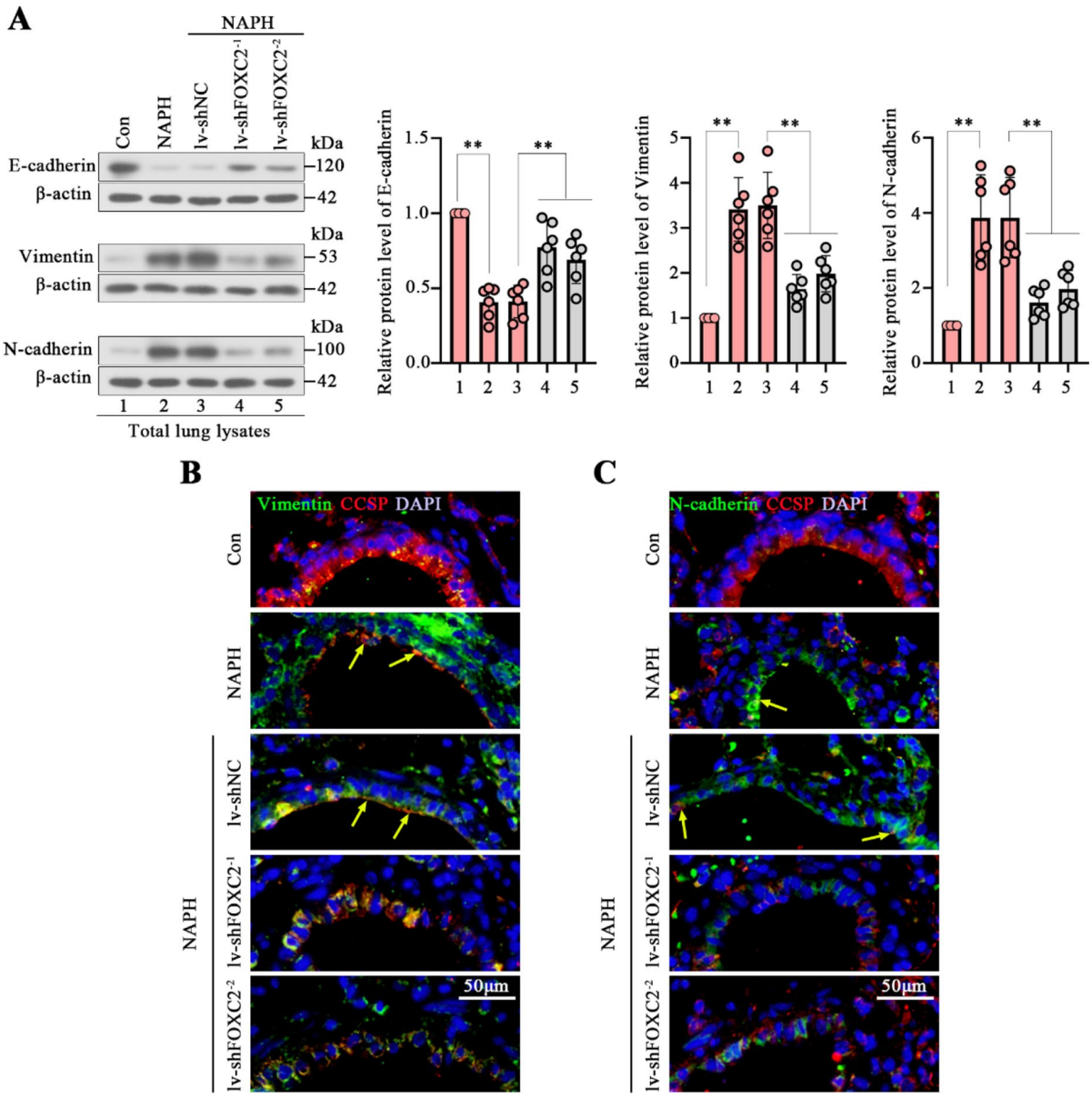

Fig. 4 Knockdown of FOXC2 suppresses EMT in NAPH-treated mice. **A** Immunoblots were performed in the lung tissues for the indicated proteins. **B** The lung tissues were stained with anti-vimentin and anti-CCSP antibodies, and representative images of dual staining were shown. Yellow arrows indicate vimentin- and CCSP-positive cells. Scale bar: 50 μm. **C** Representative images of dual immunofluorescence staining of N-cadherin and CCSP in the lung tissues. Yellow arrows indicate N-cadherin- and CCSP-positive cells. Scale bar: 50 μm. Data are presented as mean ± SD. $^{**}p < 0.01$

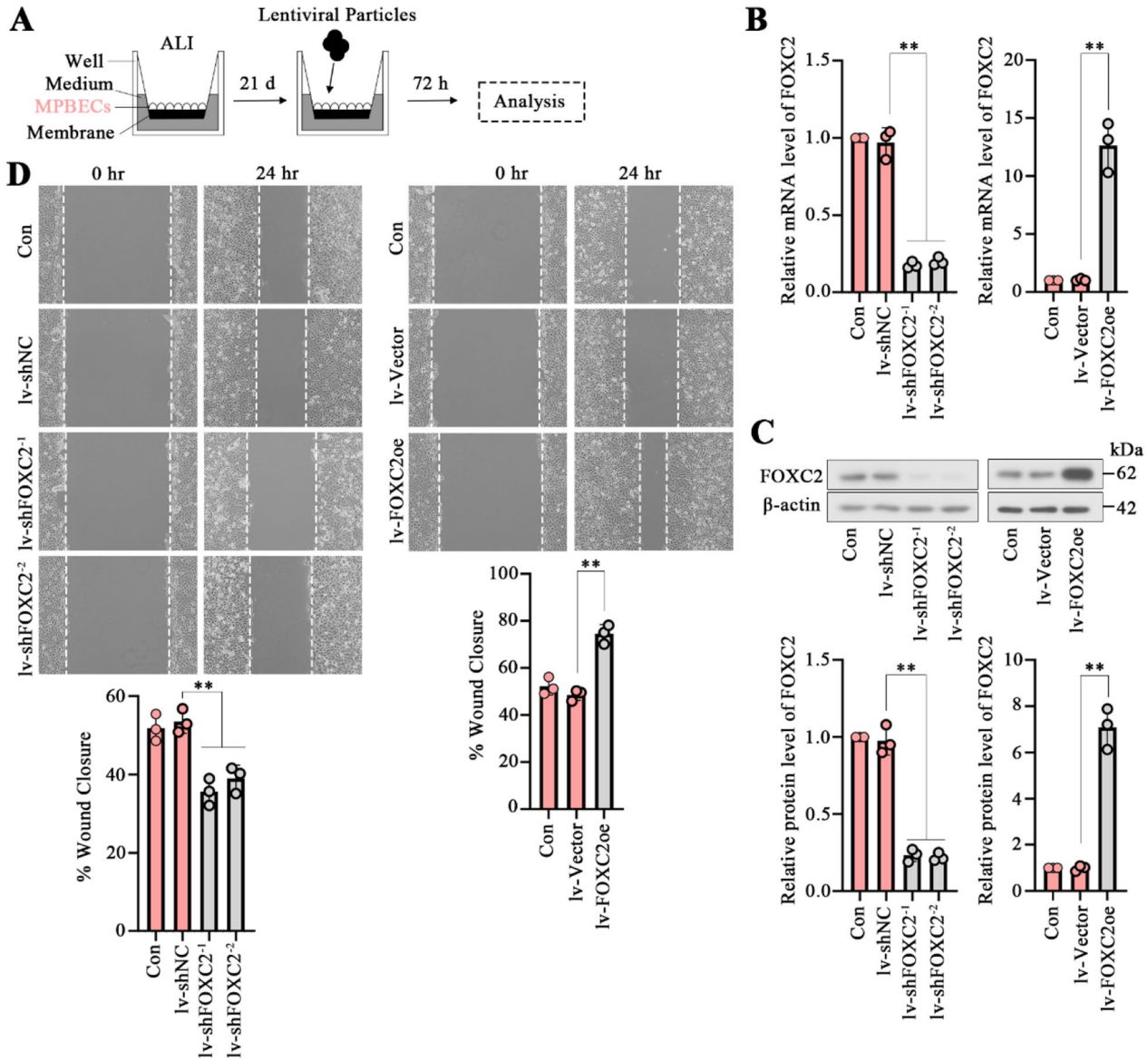

Fig. 5 Knockdown of FOXC2 inhibits migration of bronchial epithelial cells. **A** Schematic diagram of experiment in vitro. **B**, **C** The efficiency of FOXC2 knockdown and overexpression in mouse primary bronchial epithelial cells was verified using qPCR and immunoblot assays. **D** Representative images of scratch experiment and percentage of cell scratch healing. Data are presented as mean ± SD. **p < 0.01

FOXC2 mediates migration of bronchial epithelial cells

Mouse PBECs were cultured in ALI for 21 days for differentiation, and we evaluated the role of FOXC2 in PBEC migration (Fig. 5A). Infection of PBECs with lv-shFOXC2 significantly down-regulated endogenous FOXC2 mRNA and protein expression levels, while PBECs infected with lv-FOXC2oe exhibited up-regulated FOXC2 expression (Fig. 5B and C). Under normal conditions, knockdown of FOXC2 in PBECs significantly suppressed cell migration, and cell migration was increased by overexpression of FOXC2, as shown by the scratch experiment (Fig. 5D).

FOXC2 mediates EMT in mouse PBECs

Under TGF-β1-induced conditions, FOXC2 expression was up-regulated in mouse PBECs. The expression of FOXC2 in TGF-β1-induced mouse PBECs was obviously decreased by lv-shFOXC2 infection but was increased by lv-FOXC2oe. Meanwhile, knockdown of FOXC2 increased E-cadherin expression and reduced vimentin, N-cadherin and FN-EDA levels in TGF-β1-treated PBECs. Overexpression of FOXC2 exerted opposite roles in EMT markers (Fig. 6A).

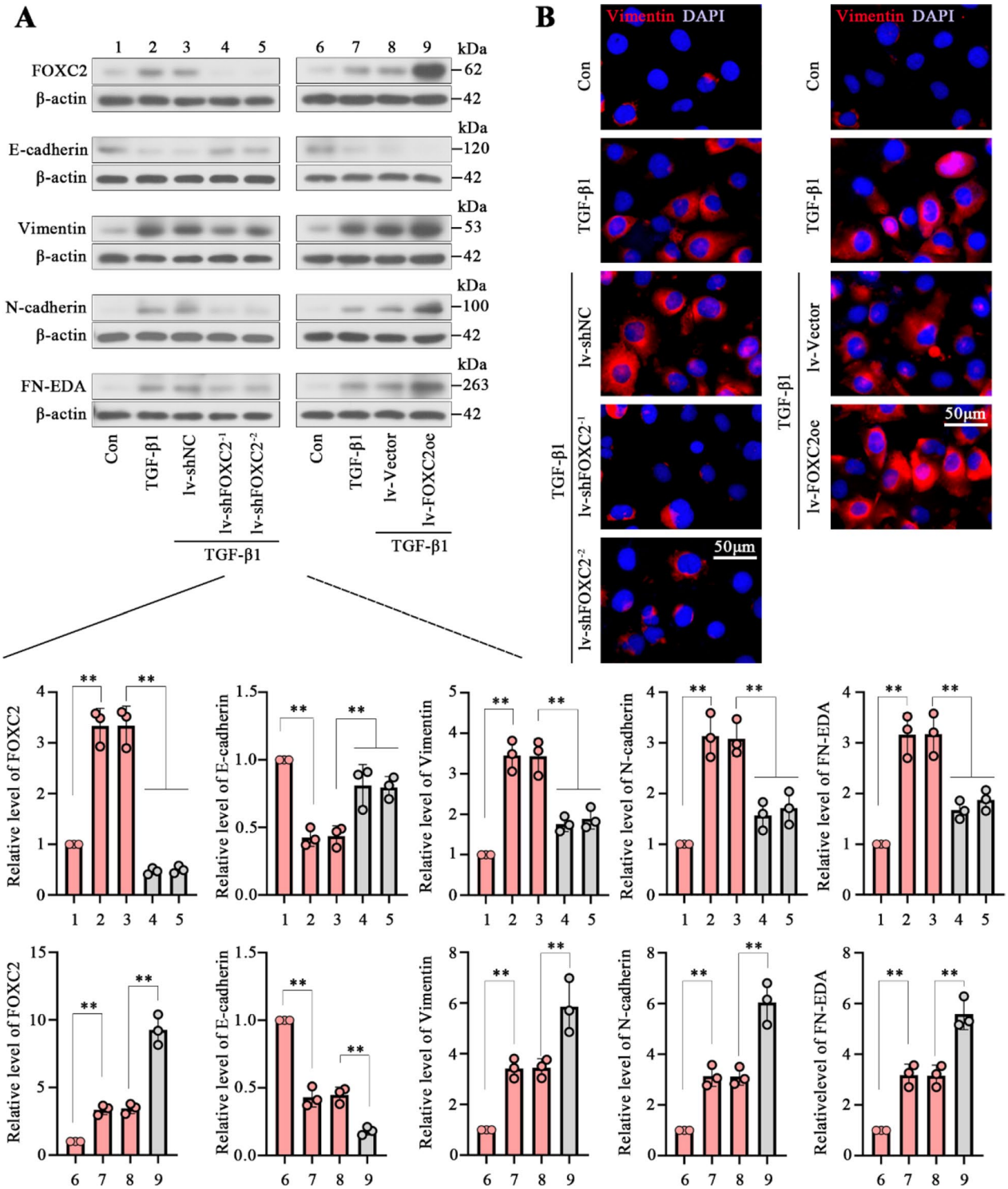

Fig. 6 Knockdown of FOXC2 inhibits EMT. **A** Immunoblot assays were performed to detect the expression of the indicated proteins in mouse primary bronchial epithelial cells. **B** Vimentin immunofluorescence staining in cells. Scale bar: 50 μm. Data are presented as mean ± SD. $^{**}p < 0.01$

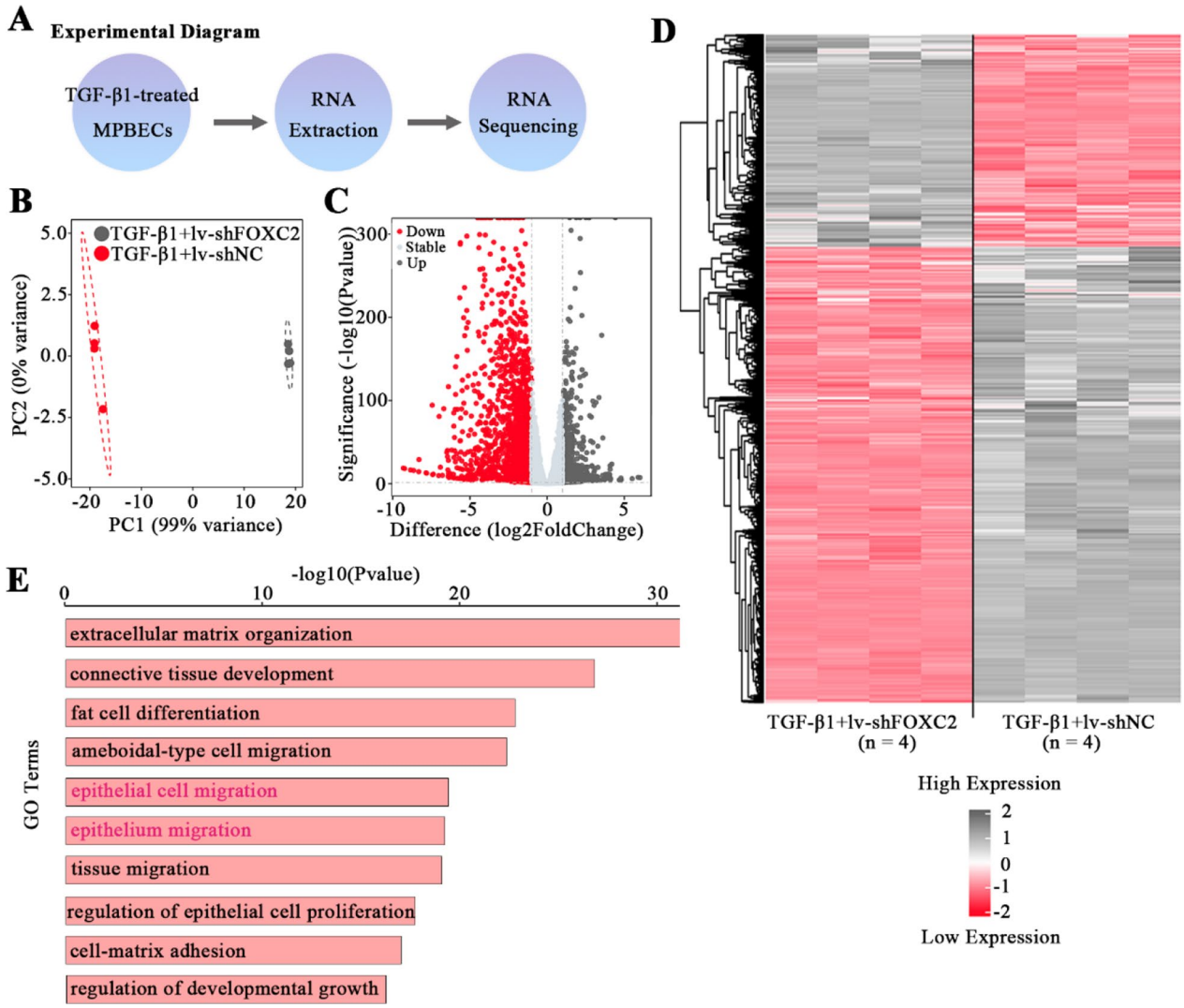

Fig. 7 FOXC2-mediated gene expression profile in TGF-β1-treated mouse primary bronchial epithelial cells. **A** Experimental diagram of mRNA sequencing (mRNA-seq). **B** PCA plot of the TGF-β1 + lv-shFOXC2 group and TGF-β1 + lv-shNC group. **C** The volcano map of all DEGs (|Log2FC|> 1 and p < 0.05). **D** Heat-map analysis of DEGs from the mRNA-seq. **E** GO functional annotation analysis of DEGs

Immunofluorescence analysis of vimentin was consistent with the result of immunoblot (Fig. 6B).

FOXC2-mediated gene expression profile in TGF-β1-induced mouse PBECs

RNA-seq analysis was conducted in TGF-β1-induced mouse PBECs to search for transcriptional targets of FOXC2. The experimental diagram was presented in Fig. 7A. As the PCA plot displayed, the segregation of two groups was evident (Fig. 7B). The data of mRNA-seq were presented using volcano map and heat-map. We identified 2490 DEGs based on the criterion of $|Log_2FC| > 1$ and $p < 0.05$ (Fig. 7C and D). The DEGs were summarized and presented in Table S1. GO enrichment results of DEGs were shown in Fig. 7E. We screened 10 GO entries, including extracellular matrix organization, connective tissue development, fat cell differentiation, ameboidal-type cell migration, epithelial cell migration, epithelium migration, tissue migration, regulation of epithelial cell proliferation, cell–matrix adhesion, and regulation of developmental growth.

ChIP-seq analysis of genomic binding sites for FOXC2

To reveal how FOXC2 controls gene expression in TGF-β1-induced mouse PBECs, ChIP-seq analysis was performed (Fig. 8A). Figure 8B showed the form and distribution of elements binding to FOXC2, including promoter, 5'UTR, 3'UTR, exon, intron, downstream region,

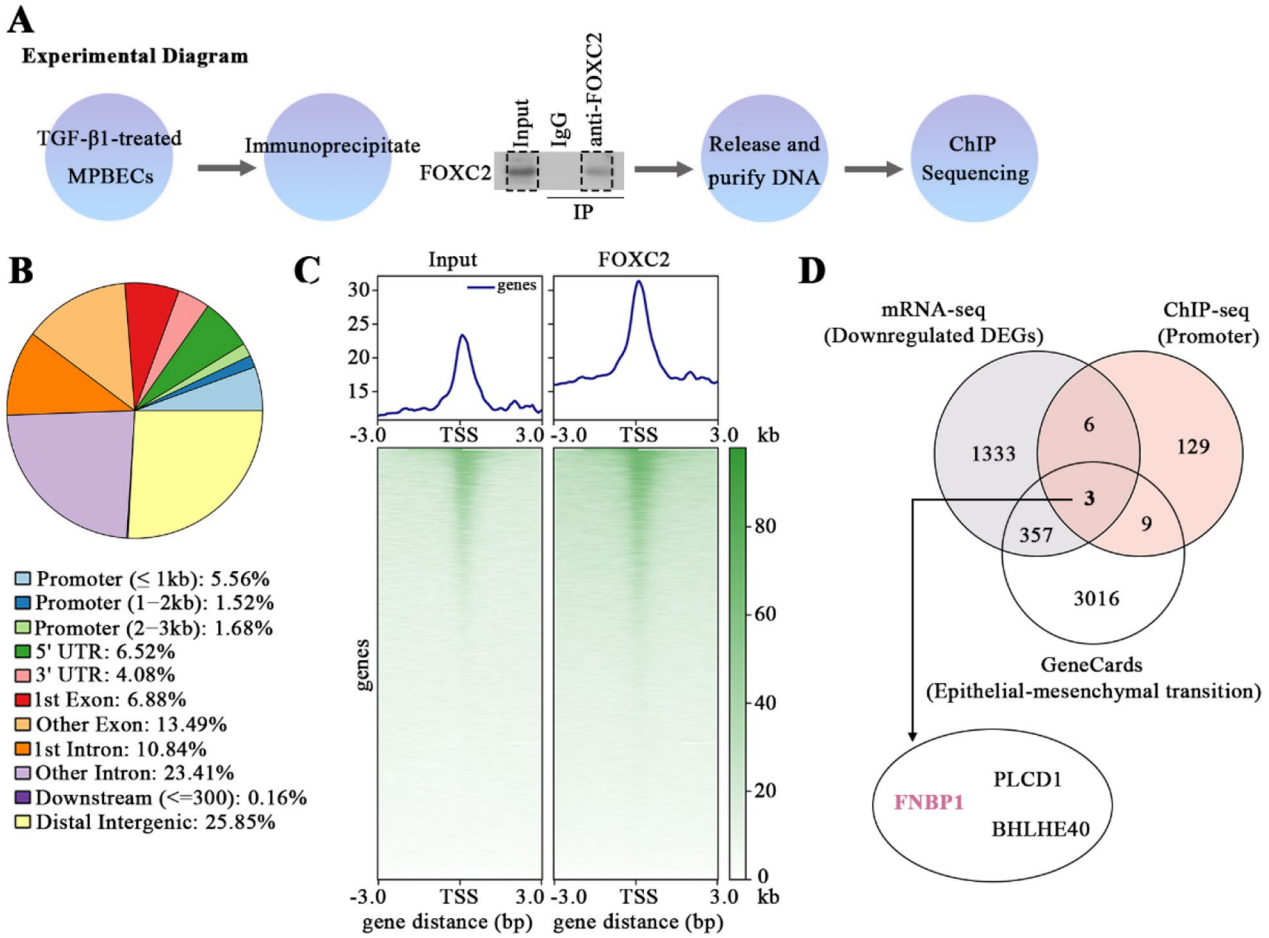

Fig. 8 FNBP1 may be a target of FOXC2 in TGF-β1-treated mouse primary bronchial epithelial cells. **A** Experimental diagram of FOXC2 ChIP sequencing (ChIP-seq). **B** Pie chart showing the distribution of FOXC2 ChIP-seq peaks on the functional elements. **C** Heat-map of the enrichment of reads near the TSS. **D** Venn diagram of mRNA-seq, ChIP-seq, and EMT-related genes from the GeneCards database

and distal intergenic sites. There was about 9% of the ChIP peaks enriched in the promoter region of target genes. The heat-map in Fig. 8C revealed that the strongest FOXC2 ChIP-seq signals were around the transcription start site (TSS). As shown in Fig. 8D, the down-regulated target DEGs related to EMT that interacted with FOXC2 were identified in PBECs. The overlapped genes in Venn diagram were FNBP1, PLCD1, and BHLHE40, and FNBP1 was highlighted for its role in EMT.

FNBP1 mediates the role of FOXC2 in EMT

The promotion of EMT process by FNBP1 has been reported in tumor cells [14], but FOXC2/FNBP1 regulatory mechanism in PBECs is not clear. Result of qPCR suggested that FOXC2 knockdown resulted in a reduction in FNBP1 mRNA level in TGF-β1-induced mouse PBECs (Fig. 9A). Dual-luciferase activity assay verified that FOXC2 overexpression increased the luciferase activity of FNBP1 promoter (Fig. 9B). In TGF-β1-induced mouse PBECs, FOXC2 could bind to FNBP1 displayed by ChIP-PCR assay (Fig. 9C). In TGF-β1-treated PBECs, FNBP1 overexpression promoted the expression of vimentin and N-cadherin inhibited by FOXC2 knockdown, as detected by immunoblot and immunofluorescence assays (Fig. 9D and E).

Discussion

In this study, we found during airway injury repair the up-regulation of FOXC2 expression to varying extents in the bronchial epithelium in response to NAPH challenge. Knockdown of FOXC2 delays epithelial regeneration after NAPH treatment in vivo. Using a mouse PBECs, we found that FOXC2 knockdown suppresses the migration and EMT, and FOXC2 overexpression exerts opposite functions in vitro. mRNA-seq and ChIP-seq analysis uncover FNBP1 as a potential target of the transcription factor FOXC2 in bronchial epithelial cells. These findings

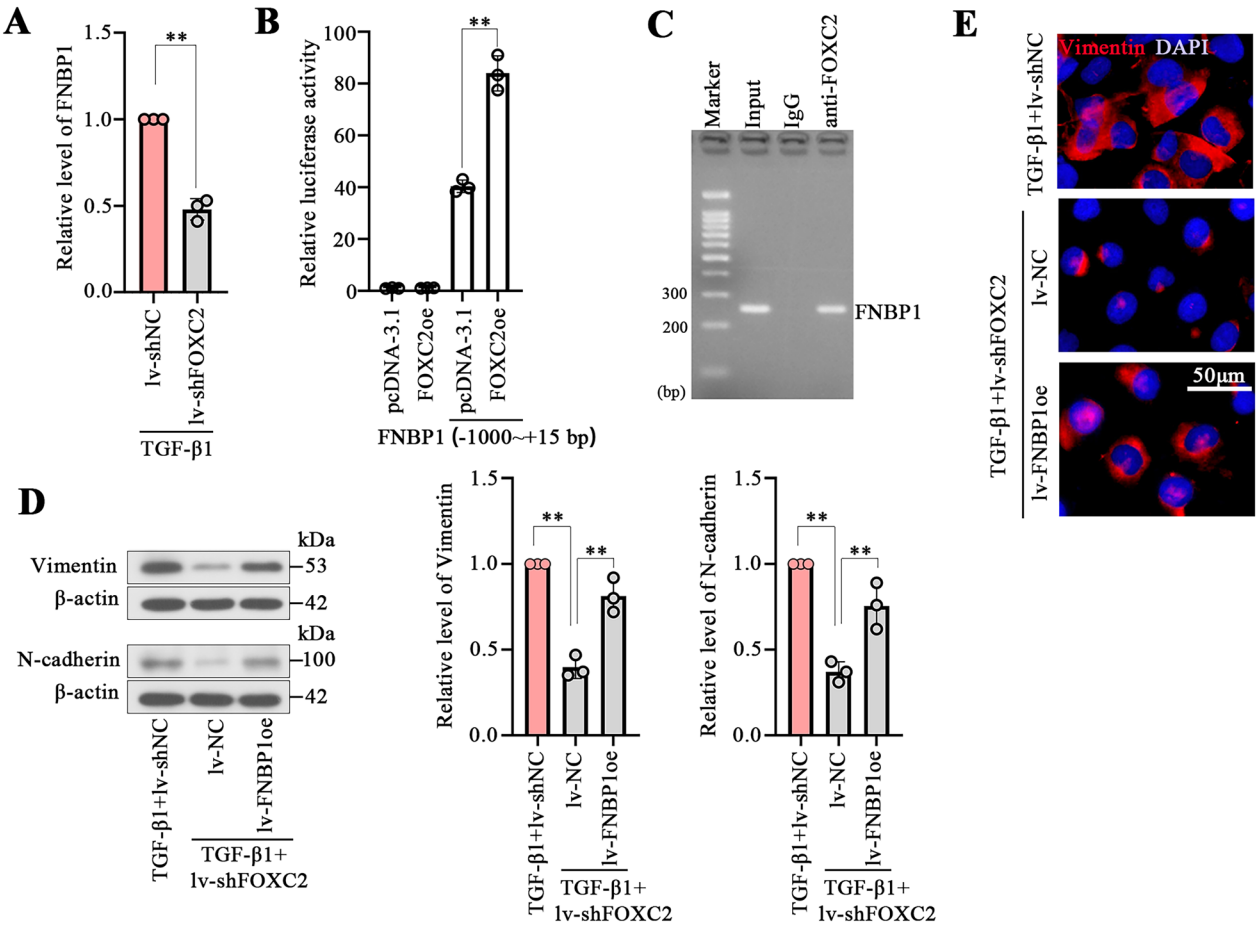

Fig. 9 FNBP1 may mediate the function of FOXC2 in TGF-β1-induced EMT. **A** qPCR analysis of FNBP1 infection efficiency in TGF-β1-treated mouse primary bronchial epithelial cells. **B** Dual-luciferase activity assay verified whether FOXC2 influences FNBP1 promoter activity in 293 T cells. **C** ChIP-PCR was conducted to confirm the interaction of FOXC2 and FNBP1 in TGF-β1-treated mouse primary bronchial epithelial cells. **D** Immunoblot analysis of vimentin and N-cadherin. **E** Representative images of immunofluorescence staining of vimentin in mouse primary bronchial epithelial cells. Scale bar: 50 μm. Values are presented as mean ± SD. $^{**}p < 0.01$

show that FOXC2 may be a critical regulator of airway repair through regulating FNBP1 transcription.

Exposure of mice to NAPH induces acute tracheal injury, a common injury model [5]. After injury, bronchial epithelial cells in the lungs, the first line of defense, are dead and gradually exfoliated. The surviving club cells act as primary progenitor cells that are responsible for restoration of the bronchiolar epithelium [22, 23]. At the early phase of injury repair, at days 2 and 3, resistant populations of club cells are activated and have the ability to migrate to denuded injury areas. By days 6 and 14, the repair phase, cell differentiation and epithelial regeneration are obvious. The bronchiolar epithelium changes are almost restored to normal at day 14 [3, 5]. Our experiments revealed the FOXC2 expression within the bronchiolar epithelium, and whether FOXC2 is implicated in the epithelium repair after injury is unclarified. The transcription factor FOXC2 has been reported to control tissue remodeling, such as vascular remodeling in adipose tissue [24] and intestinal regeneration [9]. In the present study, the down-regulated expression of FOXC2 was associated with reduced CCSP-positive club cells following exposure out to 6 days, which indicates the promoting effect of FOXC2 on cell regeneration after epithelium injury repair. Moreover, by 14 days after NAPH injury, epithelial FOXC2 knockdown delayed epithelial repair and resulted in the impairment of airway integrity. Our findings indicated that FOXC2 may be a good biomarker for airway damage in response to toxic pollutants.

Injured epithelial cells typically undergo mesenchymal transformation, accompanied by the cytoskeletal reorganization, thereby facilitating cell migration and injury repair [25]. An increasing number of researches supports that the epithelial cells after injury exhibit a dynamic variation in EMT, and EMT is a protective cellular response to injury for epithelial cells [25–27]. In

NAPH-induced injury model, EMT appears at days 2 and 3 post-NAPH [5, 28]. Previous studies have shown that FOXC2 can mediate EMT process to activate cell response after injury [10]. FOXC2 up-regulation in cancer cells enhances migration and invasion [7]. In vivo study demonstrated that FOXC2 knockdown increased epithelial marker E-cadherin and reduced mesenchymal markers vimentin and N-cadherin levels in the bronchiolar epithelium. Experimentally, EMT can be promoted by the cytokine TGF-β1 [21]. We demonstrated that FOXC2 knockdown inhibited the EMT induced by TGF-β1 using mouse primary epithelial cells. EMT in epithelium enhances the migratory ability of cells [29]. FOXC2 has been found to promote cell migration through EMT in tumors and injured kidney [7, 10]. The role of FOXC2 in epithelial cell migration in our study was consistent with the previous studies. These findings highlight the critical role of FOXC2 in epithelial repair after injury via EMT.

The potential mechanisms by which FOXC2 controls EMT progression during NAPH-induced injury of airway epithelium are incompletely understood. In our study, a combination of mRNA-seq with ChIP-seq was applied in TGF-β1-induced PBECs. The results revealed that FOXC2-regulated genes might be involved in epithelial cell migration. Comprehensive analysis of mRNA-seq, ChIP-seq and GeneCards, the FNBP1 was given more focus, which was down-regulated in TGF-β1-induced PBECs. FOXC2 can function as an activator of transcription to regulate the expression of downstream target genes [30, 31]. A recent study found that FNBP1 is required for regulating vertebrate gastrulation, involving in the modulation of cell migration [13]. Previous study has shown that FNBP1 expression was positively associated with EMT in cancer [14]. We found that FOXC2 could interact with FNBP1 and transcriptionally activate FNBP1 mRNA in mouse PBECs. Importantly, we demonstrated that increased expression of FNBP1 rescued the EMT inhibited by FOXC2 knockdown. Our results indicated the function of FOXC2 in EMT process by regulating the expression of the target FNBP1. It should be noted that we did not investigate the role of FOXC2 in human injury models, which is indeed a limitation, requiring further extended studies in the near future.

Conclusions

To conclude, the present study demonstrated that FOXC2 is a key transcription factor during NAPH-induced injury repair. FOXC2 knockdown delays the process of epithelial repair, which is closely linked to inhibited EMT and cell migration. Our study provides novel insight into epithelial cell repair after injury, and FOXC2 potentially via FNBP1 is required for epithelial cell regeneration after airway damage.

Supplementary Information

The online version contains supplementary material available at https://doi.org/10.1186/s12931-025-03150-8.

Additional file 1.

Acknowledgements
Not applicable.

Author contributions
Yudong Wang performed the experiments, analyzed the data, prepared the figures, wrote and revised the manuscript. Jun Liu conceived and designed the project and revised the manuscript. Yudong Wang and Jun Liu read and approved the final manuscript.

Funding
This study was supported by the People's Livelihood Science and Technology Program Joint Plan of Liaoning Province, China (under Grant 2021JH2/10300131).

Availability of data and materials
No datasets were generated or analysed during the current study.

Declarations

Ethics approval and consent to participate
Animal experimental protocol was approved by the Shengjing Hospital of China Medical University Institute Animal Care and Use Committee (approval number: 2024PS116K).

Consent for publication
Not applicable.

Competing interests
The authors declare no competing interests.

Author details
[1]Department of Thoracic Surgery, Shengjing Hospital of China Medical University, No. 36, Sanhao Street, Shenyang, People's Republic of China.

Received: 21 October 2024 Accepted: 11 February 2025
Published online: 10 March 2025

References

1. Lambrecht BN, Hammad H. The airway epithelium in asthma. Nat Med. 2012;18:684–92.
2. Varricchi G, Brightling CE, Grainge C, Lambrecht BN, Chanez P. Airway remodelling in asthma and the epithelium: on the edge of a new era. Eur Respir J. 2024;63:2301619.
3. Carratt SA, Kovalchuk N, Ding X, Van Winkle LS. Metabolism and lung toxicity of inhaled naphthalene: effects of postnatal age and sex. Toxicol Sci. 2019;170:536–48.
4. Lafkas D, Shelton A, Chiu C, de Leon BG, Chen Y, Stawicki SS, Siltanen C, Reichelt M, Zhou M, Wu X, et al. Therapeutic antibodies reveal Notch control of transdifferentiation in the adult lung. Nature. 2015;528:127–31.
5. Gorissen SH, Hristova M, Habibovic A, Sipsey LM, Spiess PC, Janssen-Heininger YM, van der Vliet A. Dual oxidase-1 is required for airway epithelial cell migration and bronchiolar reepithelialization after injury. Am J Respir Cell Mol Biol. 2013;48:337–45.
6. Inman KE, Caiaffa CD, Melton KR, Sandell LL, Achilleos A, Kume T, Trainor PA. Foxc2 is required for proper cardiac neural crest cell

migration, outflow tract septation, and ventricle expansion. Dev Dyn. 2018;247:1286–96.
7. Sarkar PL, Lee W, Williams ED, Lubik AA, Stylianou N, Shokoohmand A, Lehman ML, Hollier BG, Gunter JH, Nelson CC. Insulin enhances migration and invasion in prostate cancer cells by up-regulation of FOXC2. Front Endocrinol (Lausanne). 2019;10:481.
8. Pham TND, Perez White BE, Zhao H, Mortazavi F, Tonetti DA. Protein kinase C α enhances migration of breast cancer cells through FOXC2-mediated repression of p120-catenin. BMC Cancer. 2017;17:832.
9. Tan C, Norden PR, Yu W, Liu T, Ujiie N, Lee SK, Yan X, Dyakiv Y, Aoto K, Ortega S, et al. Endothelial FOXC1 and FOXC2 promote intestinal regeneration after ischemia-reperfusion injury. EMBO Rep. 2023;24: e56030.
10. Hader C, Marlier A, Cantley L. Mesenchymal-epithelial transition in epithelial response to injury: the role of Foxc2. Oncogene. 2010;29:1031–40.
11. Tsuji M, Morishima M, Shimizu K, Morikawa S, Heglind M, Enerbäck S, Ezaki T, Tamaoki J. Foxc2 influences alveolar epithelial cell differentiation during lung development. Dev Growth Differ. 2017;59:501–14.
12. Zhang J, Li X, Zhou Y, Lin M, Zhang Q, Wang Y. FNBP1 facilitates cervical cancer cell survival by the constitutive activation of FAK/PI3K/AKT/mTOR signaling. Cells. 1964;2023:12.
13. Zeni C, Komiya Y, Habas R. Formin binding protein 1 (FNBP1) regulates non-canonical Wnt signaling and vertebrate gastrulation. Dev Biol. 2024;515:18–29.
14. Yoon BK, Hwang N, Chun KH, Lee Y, Duarte TPM, Kim JW, Kim TH, Cheong JH, Fang S, Kim JW. Sp1-induced FNBP1 drives rigorous 3D cell motility in EMT-type gastric cancer cells. Int J Mol Sci. 2021;22:6784.
15. Chen P, McGuire JK, Hackman RC, Kim KH, Black RA, Poindexter K, Yan W, Liu P, Chen AJ, Parks WC, Madtes DK. Tissue inhibitor of metalloproteinase-1 moderates airway re-epithelialization by regulating matrilysin activity. Am J Pathol. 2008;172:1256–70.
16. Tang PC, Chung JY, Xue VW, Xiao J, Meng XM, Huang XR, Zhou S, Chan AS, Tsang AC, Cheng AS, et al. Smad3 promotes cancer-associated fibroblasts generation via macrophage-myofibroblast transition. Adv Sci (Weinh). 2022;9: e2101235.
17. Zhang G, He P, Gaedcke J, Ghadimi BM, Ried T, Yfantis HG, Lee DH, Hanna N, Alexander HR, Hussain SP. FOXL1, a novel candidate tumor suppressor, inhibits tumor aggressiveness and predicts outcome in human pancreatic cancer. Cancer Res. 2013;73:5416–25.
18. Morimoto M, Liu Z, Cheng HT, Winters N, Bader D, Kopan R. Canonical Notch signaling in the developing lung is required for determination of arterial smooth muscle cells and selection of Clara versus ciliated cell fate. J Cell Sci. 2010;123:213–24.
19. Shan L, Chen L, Shen W, Zhou Q, Liu S, Han L, Zhang Q, Dai B, Zhao Y. FOXK2 facilitates the airway remodeling during chronic asthma by promoting glycolysis in a SIRT2-dependent manner. Faseb j. 2024;38: e23756.
20. Miyashita N, Horie M, Suzuki HI, Saito M, Mikami Y, Okuda K, Boucher RC, Suzukawa M, Hebisawa A, Saito A, Nagase T. FOXL1 regulates lung fibroblast function via multiple mechanisms. Am J Respir Cell Mol Biol. 2020;63:831–42.
21. Kalluri R, Weinberg RA. The basics of Epithelial–mesenchymal transition. J Clin Invest. 2009;119:1420–8.
22. Rackley CR, Stripp BR. Building and maintaining the epithelium of the lung. J Clin Invest. 2012;122:2724–30.
23. Martinu T, Todd JL, Gelman AE, Guerra S, Palmer SM. Club cell secretory protein in lung disease: emerging concepts and potential therapeutics. Annu Rev Med. 2023;74:427–41.
24. Xue Y, Cao R, Nilsson D, Chen S, Westergren R, Hedlund EM, Martijn C, Rondahl L, Krauli P, Walum E, et al. FOXC2 controls Ang-2 expression and modulates angiogenesis, vascular patterning, remodeling, and functions in adipose tissue. Proc Natl Acad Sci U S A. 2008;105:10167–72.
25. Do AR, Ko DY, Kim J, Bak SH, Lee KY, Yoon D, Shin C, Kim S, Kim WJ, Won S. Genome-wide association study of airway wall thickening in a Korean chronic obstructive pulmonary disease cohort. Genes (Basel). 2022;13:1258.
26. Han L, Luo H, Huang W, Zhang J, Wu D, Wang J, Pi J, Liu C, Qu X, Liu H, et al. Modulation of the EMT/MET process by E-cadherin in airway epithelia stress injury. Biomolecules. 2021;11:669.
27. Tan ML, Huang WJ, Wang Y, Liu L, Pan Y, Li JJ, Zhang J, Ouyang M, Qu XP, Liu HJ, et al. Integrin-β4 regulates the dynamic changes of phenotypic characteristics in association with Epithelial–mesenchymal transition (EMT) and RhoA activity in airway epithelial cells during injury and repair. Int J Biol Sci. 2022;18:1254–70.
28. Mottais A, Riberi L, Falco A, Soccal S, Gohy S, De Rose V. Epithelial–mesenchymal transition mechanisms in chronic airway diseases: a common process to target? Int J Mol Sci. 2023;24:12412.
29. Lee HW, Jose CC, Cuddapah S. Epithelial–mesenchymal transition: insights into nickel-induced lung diseases. Semin Cancer Biol. 2021;76:99–109.
30. Park SJ, Gadi J, Cho KW, Kim KJ, Kim SH, Jung HS, Lim SK. The forkhead transcription factor Foxc2 promotes osteoblastogenesis via up-regulation of integrin β1 expression. Bone. 2011;49:428–38.
31. Hayashi H, Sano H, Seo S, Kume T. The Foxc2 transcription factor regulates angiogenesis via induction of integrin beta3 expression. J Biol Chem. 2008;283:23791–800.

Publisher's Note